

# Allegro Memo No. 2: AGB stars as calibrators for HIFI and ALMA

Christophe Risacher & Floris van der Tak

SRON Netherlands Institute for Space Research  
Landleven 12, 9747 AD Groningen, The Netherlands

risacher@sron.nl; vdtak@sron.nl

December 2009

## Abstract

We present observations of the CO 6-5 line toward 20 AGB stars with the CHAMP+ instrument at the APEX telescope. The intensities of 1.3–81 K have uncertainties of  $\approx 15\%$  and may be used as a calibration scale for HIFI and ALMA. Except IRC+10216, the sources may also be compact enough for ALMA phase calibration.

## Contents

<b>1 Motivation and source selection</b>	<b>2</b>
<b>2 Observations and results</b>	<b>2</b>
<b>3 Calibration and uncertainty</b>	<b>2</b>
<b>4 Source size and phase calibration</b>	<b>4</b>
<b>5 Conclusions and future work</b>	<b>4</b>

# 1 Motivation and source selection

The calibration of astronomical observations is necessary to compare measurements taken at different times, with different telescopes, or at different wavelengths. Calibrating single-dish submillimeter telescopes including Herschel/HIFI requires a set of astronomical sources with a known high line or continuum brightness which are spread over the sky (Ossenkopf 2003). In the case of interferometers such as ALMA, calibration has more aspects (Laing 2006), but the flux and phase calibration are the most challenging, especially at high frequencies (Van der Tak 2009). This report presents observations of 20 AGB stars in the CO  $J=6\rightarrow 5$  line. The sources have been selected on high brightness in low- $J$  CO lines from Kerschbaum & Olofsson (1999), Sahai & Liechti (1995), Young (1995), Olofsson et al (1993) and Ryde et al (1999).

# 2 Observations and results

The observations were done during several runs in November 2008, July 2009 and October 2009 at the APEX telescope (Güsten et al 2006). The CHAMP+ receiver is a 2-colour multibeam receiver centered at the 690 and 810 GHz windows (Güsten et al 2008).

Two main modes of observing were considered. In the initial observing runs, small maps were made in a hexagonal pattern of size  $40''\times 40''$ . The Appendix presents some of those maps. As only the central pixel sees the source, this mapping mode is not very efficient. Therefore, in later observing runs, only peak-up observations were done. Once the telescope was pointed, a long integration was performed to reach a high S/N. In almost all cases, the telescope pointing was done on the source itself using a cross of 5 by 5 points. The telescope focus was normally done on a planet.

The receiver temperatures for the CHAMP+ array are typically  $\approx 400$  K SSB for the CO 6-5 tuning. All observations were typically done with precipitable water vapour (PWV) levels between 0.2 and 0.6 mm. This is equivalent to a system temperature between 1000-3000 K for the source elevations of 30 to 70 degrees. The integration times range from 1 minute for the brightest sources to 10 minutes for the weakest ones.

The backend configuration uses two FFTS modules with a bandwidth of 1.4 GHz, which are combined with a small overlap region yielding a total backend coverage of 2.4 GHz. The backend resolution is either 1024, 2048, 4096 or 8192 channels, equivalent to a  $\Delta V$  of  $0.08 \text{ km s}^{-1}$ ,  $0.16 \text{ km s}^{-1}$ ,  $0.32 \text{ km s}^{-1}$  or  $0.64 \text{ km s}^{-1}$ .

The data were reduced with the CLASS software using standard procedures. Table 1 gives the results, while Table 2 gives the observing log. The last column of Table 1 gives the spectral resolution applicable to that observation. The observed intensities assume a sideband gain of 14 dB as measured in August 2009 by the instrument team.

# 3 Calibration and uncertainty

The calibration of the data was done using external Hot and Cold loads at physical temperatures of 285 K and 75 K. This hot/cold calibration was done typically every 5-10 minutes. The telescope staff and the instrument team have observed planets to allow estimating the beam efficiencies (Güsten et al 2008). Mars, Jupiter and Uranus were observed during the runs, but we use only Mars to estimate the efficiencies, since Jupiter is much more extended than our sources and Uranus is too weak. The measure-

ments indicate a value of  $\eta_{\text{mb}}=0.42 \pm 0.02$  where the error bar represents the variation in  $\eta_{\text{mb}}$  from run to run. See the CHAMP+ calibration weblog<sup>1</sup> for further details.

The different contributions to the calibration uncertainty are :

1. Beam efficiency: repeated observations during different runs indicate an uncertainty of 5% as discussed above.
2. Hot and cold loads: The intensity scale is proportional to  $(J_{\nu}(\text{hot}) - J_{\nu}(\text{cold}))$ , where  $J_{\nu}(T)$  is the radiation field at the observing frequency  $\nu$ , equal to  $\eta_c B_{\nu}(T)$  where  $\eta_c$  is the coupling efficiency and  $B_{\nu}(T)$  is the Planck function at the load temperature. The temperature sensors on the loads are accurate to better than 1 K, and the beam coupling to the loads has been measured during commissioning and is assumed to be stable. Possible systematic effects are temperature gradients between the sensors and the actual blackbody, and standing waves coming from reflection off the liquid nitrogen surface and the blackbody itself. Assuming that these are minor effects, we estimate an upper limit on this error source of 5%.
3. Sideband ratio: The image sideband is filtered out with a Martin-Pupplett interferometer. The achieved rejection is better than 10 dB across the IF band, and is likely to be >15–20 dB for the CO 6-5 line at the IF band center. A fraction  $\eta_{\text{sb}}$  of the line peak is measured, with  $\eta_{\text{sb}}=0.95\text{--}0.99$ , leading to a 5% calibration uncertainty.
4. Pointing accuracy: The absolute pointing accuracy of the APEX telescope is 3–4'', but the pointing was corrected before each of our observations, it should be accurate to 1–2''. For point-like emission in a Gaussian telescope beam with FWHM = 10'', an 1'' offset reduces the intensity by 2.5% and a 2'' offset by 10%. Thus pointing again introduces a 5% uncertainty.
5. The atmospheric model: It is difficult to estimate the intrinsic accuracy of the model used at the telescope to estimate the atmospheric opacity from the sky brightness (Pardo et al 2001), so we give an empirical estimate. The line intensities in the two backend sections differ by 5–10%, due to the presence of a strong atmospheric absorption feature in one subband that was not fitted properly by the atmospheric model. Averaging the two subbands reduces this error to about  $\pm 5\%$ .

We estimate the overall calibration uncertainty as the quadratic sum of these contributions, which is 11%, or 15% when allowing for systematic effects.

Some of the sources were observed at several opportunities, and typical variations are of the order of 5-10%. Larger variations are found when sources are observed during day-time. Those measurements are less reliable as rapid temperature changes affect the dish shape and specially the focus position, and even a small z-focus variation is noticeable. Therefore if a focus was not performed shortly before the observation, we consider the result unreliable. The repeated observations indeed show this effect, with lower fluxes in those cases.

---

<sup>1</sup><http://www.mpi.fr.de/div/submmtech/heterodyne/champplus/champmain.html>

## 4 Source size and phase calibration

The suitability of our sources as phase calibrators for ALMA depends on the size of the emitting region. This size is unknown; an upper limit is given by the size of the  $J=2-1$  emission which has been measured with the Submillimeter Array towards VY CMa,  $\pi^1$  Gru and V Hya to be  $5-10''$  (Hirano et al 2004; Chiu et al 2006; Muller et al 2007). The one exception is IRC+10216 whose envelope extends over  $\gtrsim 10''$  (e.g., Schöier et al 2007). For this source, the Jupiter efficiency may actually be preferred over the Mars value; however, we prefer to present one consistent set of measurements in Table 1.

The size of the 6-5 emission may be estimated by comparing our measured intensities with those by Kemper et al (2003) who used the JCMT with an  $8''$  beam. In the case of VY CMa, Kemper et al measured  $T_{\text{mb}} = 4.4$  K, and the intensity ratio with APEX of 1.63 is consistent with the value of 1.56 expected if the emission is unresolved with both telescopes (size  $\lesssim 1''$ ). This estimate is in agreement with the following more theoretical line of thought. In the model by Muller et al (2007) for the envelope of VY CMa, the temperature reaches 83 K (the location of the  $J=6$  level of CO) at a radius of  $3 \times 10^{16}$  cm, which corresponds to  $1''.33$  at a distance of 1.5 kpc.

We consider the size of the VY CMa envelope as an upper limit for the other stars, since VY CMa has one of the highest known mass loss rates among AGB stars (e.g., Polehampton et al 2009). However, for WX Psc, Kemper et al measured an intensity of 2.3 K, which is below the APEX value. Maybe this source is variable, or the emission is spatially resolved with the JCMT. This source should be re-observed. Unfortunately, VY CMa and WX Psc are the only sources which have been observed with JCMT and APEX.

## 5 Conclusions and future work

With main beam temperatures of  $\gtrsim 1$  K, our sources are detectable in a minute, which is bright enough to serve as flux calibrators for HIFI Band 2 and ALMA Band 9. With the exception of IRC+10216, the sources may be compact enough for ALMA phase calibration, and we recommend that the ALMA Calibrator Survey includes these objects to find out.

In the future, we plan to augment this list with more stars to improve the sky coverage. We also plan more monitoring of selected stars to assess whether variability is significant, which would be a problem for flux calibration. The CO emission originates far out in the stellar wind, and variability on timescales of days or weeks are unlikely, while variations on timescales of months or years are quite possible. Finally we plan to present observations of the CO  $J=7-6$  line of the same stars, which may be used to calibrate HIFI Band 3 and ALMA Band 10.

## Acknowledgements

The authors thank the APEX staff and the CHAMP+ team for their support, especially Rolf Güsten and Friedrich Wyrowski (MPIfR).

## References

- Chiu et al 2006: ApJ 645, 605  
Güsten et al 2006: A&A 454, L13  
Güsten et al 2008: Proc. SPIE 7020, 25  
Hirano et al 2004: ApJ 616, L43  
Kerschbaum & Olofsson 1999: A&AS 138, 299  
Laing 2006: ALMA Commissioning and Science Verification Plan  
Muller et al 2007: ApJ 656, 1109  
Olofsson et al 1993: ApJS 87, 267  
Ossenkopf 2003: The intensity calibration for HIFI, ALMA Memo 442  
Pardo et al 2001: IEEE Trans. on Antennas and Propagation, 49/12, 1683  
Polehampton et al 2009: A&A, in press; arXiv 0912/1626  
Ryde et al 1999: A&A 345, 841  
Sahai & Liechti 1995: A&A 293, 198  
Schöier et al 2007: ApJ 670, 766  
Young 1995: ApJ 445, 872

Table 1:  $^{12}\text{CO}$  ( $J = 6-5$ ) observations of a selected list of AGB stars. The line position and FWHM are also presented. The  $T_{MB}$  (K) assumes a beam efficiency of 0.42, and the error bars presented are the  $1\sigma$  rms values.

Source	$T_{MB}$ (K)	$V_{\text{LSR}}$ $\text{km s}^{-1}$	FWHM $\text{km s}^{-1}$	$\Delta\nu$ $\text{km s}^{-1}$
IRC+10216	$81.0 \pm 1.75$	-25.6	18.7	0.16
O Cet	$34.5 \pm 0.75$	+46.8	4.8	0.16
R Dor	$17.1 \pm 0.33$	+7.3	9.1	0.64
Ep Aqr	$9.3 \pm 0.53$	-33.7	1.9	0.16
L2 Pup	$7.7 \pm 0.27$	+33.4	3.44	0.64
RAFGL 3068	$7.6 \pm 0.56$	-30.8	16.6	0.16
R Hor	$7.1 \pm 0.50$	+37.3	6.04	0.64
IRAS15194-5115	6.92.03	-15.5	29.1	0.64
IK Tau	$6.6 \pm 0.76$	+34.7	24.2	0.64
R And	$6.3 \pm 0.91$	-15.2	10.5	0.16
V Hya	$6.3 \pm 1.09$	-17.0	24.9	0.32
07454-7112	$6.2 \pm 0.82$	-38.9	15.3	0.16
W Aql	$6.1 \pm 1.12$	-23.1	36.7	0.64
$\pi^1$ Gru	$5.7 \pm 0.70$	-11.2	16.7	0.64
TX Psc	$4.4 \pm 1.00$	+12.7	2.1	0.64
VY CMa	$2.8 \pm 0.76$	+26.5	53.9	0.64
WX Psc	$2.4 \pm 0.35$	+9.6	24.2	0.32
R Scl	$1.5 \pm 0.33$	-19.4	23.0	0.32
R For	$1.3 \pm 0.20$	-3.1	22.7	0.32
V1943 Sgr	$1.3 \pm 0.08$	-15.2	7.3	0.64

Table 2: Source list and observing dates with corresponding APEX scan numbers

Source	$\alpha_{2000}$	$\delta_{2000}$	Date	Scans
IRC+10216	09 <sup>h</sup> 47 <sup>m</sup> 57.3 <sup>s</sup>	+13°16'42.9"	11 Nov 2008	61419
O Cet	02 <sup>h</sup> 19 <sup>m</sup> 20.8 <sup>s</sup>	-02°58'40.9"	21 Oct 2009	73248
R Dor	04 <sup>h</sup> 36 <sup>m</sup> 45.6 <sup>s</sup>	-62°04'37.8"	10 Nov 2008	60930 – 60932
Ep Aqr	21 <sup>h</sup> 46 <sup>m</sup> 31.9 <sup>s</sup>	-02°12'45.8"	23 Oct 2009	73576 – 73577
L2 Pup	07 <sup>h</sup> 13 <sup>m</sup> 32.3 <sup>s</sup>	-44°38'23.1"	11 Nov 2008	61346
RAFGL 3068	23 <sup>h</sup> 19 <sup>m</sup> 12.4 <sup>s</sup>	+17°11'35.4"	23 Oct 2009	73582 – 73584
R Hor	02 <sup>h</sup> 53 <sup>m</sup> 52.8 <sup>s</sup>	-49°53'22.7"	10 Nov 2008	60949 – 60951
IRAS 15194-5115	15 <sup>h</sup> 23 <sup>m</sup> 04.9 <sup>s</sup>	-51°25'59.0"	17 Jun 2009	33215
IK Tau	03 <sup>h</sup> 53 <sup>m</sup> 28.8 <sup>s</sup>	+11°24'22.6"	22 Oct 2009	73253
R And	00 <sup>h</sup> 24 <sup>m</sup> 01.9 <sup>s</sup>	+38°34'37.1"	24 Oct 2009	73965 – 73970
V Hya	10 <sup>h</sup> 51 <sup>m</sup> 37.2 <sup>s</sup>	-21°15'00.3"	11 Nov 2008	61365
07454-7112	07 <sup>h</sup> 45 <sup>m</sup> 02.8 <sup>s</sup>	-71°19'42.2"	11 Nov 2008	61378 – 61408
W Aql	19 <sup>h</sup> 15 <sup>m</sup> 23.4 <sup>s</sup>	-07°02'49.9"	21 Oct 2009	73141 – 73147
$\pi^1$ Gru	22 <sup>h</sup> 22 <sup>m</sup> 44.2 <sup>s</sup>	-45°56'52.6"	17 Jun 2009	33353 – 33357
VY CMa	07 <sup>h</sup> 22 <sup>m</sup> 58.3 <sup>s</sup>	-25°46'03.2"	17 Jun 2009	33432
TX Psc	23 <sup>h</sup> 46 <sup>m</sup> 23.5 <sup>s</sup>	+03°29'12.4"	24 Oct 2009	73716 – 73917
WX Psc	01 <sup>h</sup> 06 <sup>m</sup> 26.0 <sup>s</sup>	+12°35'53.0"	24 Oct 2009	73924 – 73959
R Scl	01 <sup>h</sup> 26 <sup>m</sup> 58.1 <sup>s</sup>	-32°32'35.5"	23 Oct 2009	73591 – 73593
R For	02 <sup>h</sup> 29 <sup>m</sup> 15.3 <sup>s</sup>	-26°05'55.7"	24 Oct 2009	73978 – 73984
V1943 Sgr	20 <sup>h</sup> 06 <sup>m</sup> 55.2 <sup>s</sup>	-27°13'29.8"	14 Sep 2008	46122 – 46140

9226; 1 IRC+10216 CO(6-5) AP-C604-AF02 0:11-NOV-2008 R:11-NOV-2008  
 RA: 09:47:57.29 DEC: 13:16:42.8 Eq 2000.0 Offs: +0.0 +0.0  
 Unknown tau: 0.640 Tsys: 1251. Time: 0.33 min El: 46.8  
 N: 6608 lO: 3304.39 V0: -25.00 Dv: 0.1588 LSR  
 F0: 691473.062 Df: -0.3662 Fi: 679474.971  
 Bef: 1.0 Fef: 0.95 Gim: 0.1000  
 H2O : 0.4210 Pamb: 554.3 Tamb: 272.6 Tchop: 289.2 Tcold: 72.6  
 Tatm: 0.0 Tau: 0.640 Tatm i: 0.0 Tau i: 0.491  
 61419,

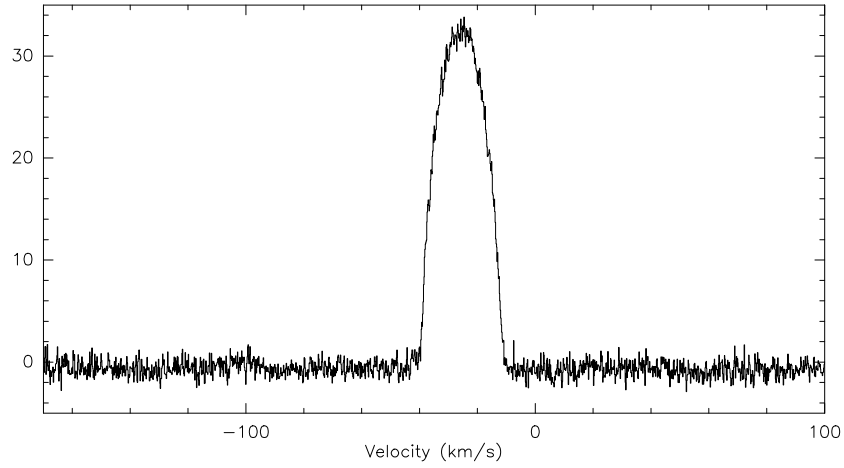


Figure 1: IRC+10216 CO(6-5) spectrum

213980; 2 O-Ceti CO(6-5) AP-C604-AF02 0:22-OCT-2009 R:25-OCT-2009  
 RA: 02:19:20.79 DEC: -02:58:40.9 Eq 2000.0 Offs: -0.3 -0.1  
 Unknown tau: 0.817 Tsys: 1332. Time: 2.5 min El: 63.6  
 N: 6607 lO: 3304.14 V0: 46.00 Dv: 0.1588 LSR  
 F0: 691473.076 Df: -0.3662 Fi: 679470.871  
 Bef: 1.0 Fef: 0.95 Gim: 0.1000  
 H2O : 0.5728 Pamb: 554.5 Tamb: 269.3 Tchop: 288.4 Tcold: 72.6  
 Tatm: 0.0 Tau: 0.817 Tatm i: 0.0 Tau i: 0.668  
 73248,

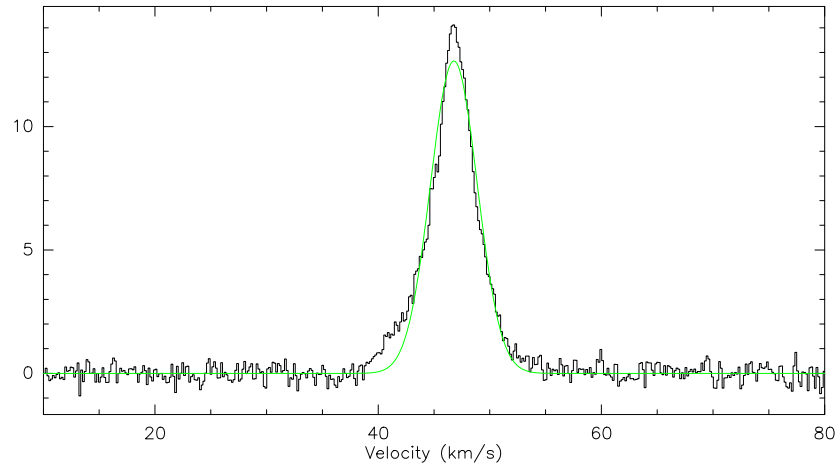


Figure 2: O-Ceti CO(6-5) spectrum



1026; 1 R-DOR CO(6-5) AP-C604-AF02 O:10-NOV-2008 R:10-NOV-2008  
 RA: 04:36:45.60 DEC: -62:04:38.0 Eq 2000.0 Offs: -0.2 -0.4  
 Unknown tau: 0.718 Tsys: 1430. Time: 7.4 min El: 43.3  
 N: 1652 l0: 826.473 V0: 7.100 Dv: 0.6351 LSR  
 F0: 691473.062 Df: -1.465 Fi: 679472.006  
 Bef: 1.0 Fef: 0.95 Gim: 0.1000  
 H2O : 0.4695 Pamb: 554.4 Tamb: 271.4 Tchop: 289.3 Tcold: 72.7  
 Tاتم: 0.0 Tau: 0.718 Tاتم i: 0.0 Tau i: 0.548  
 60930, 60932,

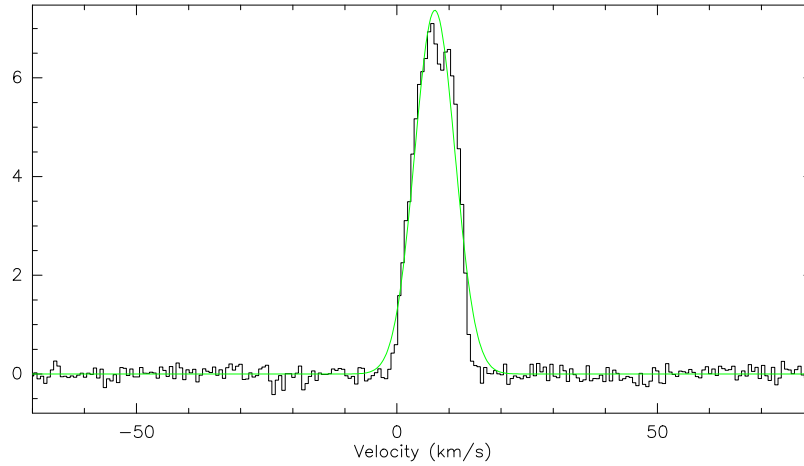


Figure 3: R-DOR CO(6-5) spectrum

1096; 1 EP-AQR CO(6-5) AP-C604-AF02 O:23-OCT-2009 R:23-OCT-2009  
 RA: 21:46:31.86 DEC: -02:12:45.8 Eq 2000.0 Offs: -0.1 -0.1  
 Unknown tau: 0.667 Tsys: 1125. Time: 4.0 min El: 53.2  
 N: 6608 l0: 3304.39 V0: -34.00 Dv: 0.1588 LSR  
 F0: 691473.076 Df: -0.3662 Fi: 679473.758  
 Bef: 1.0 Fef: 0.95 Gim: 0.1000  
 H2O : 0.4346 Pamb: 553.7 Tamb: 270.6 Tchop: 288.4 Tcold: 72.6  
 Tاتم: 0.0 Tau: 0.667 Tاتم i: 0.0 Tau i: 0.515  
 73576- 73577,

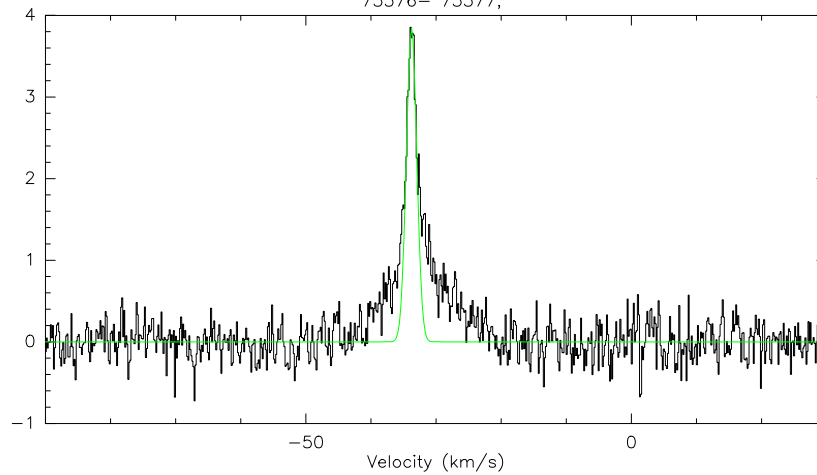


Figure 4: EP-AQR CO(6-5) spectrum

2006; 1 L2-PUP CO(6-5) AP-C604-AF02 O:11-NOV-2008 R:11-NOV-2008  
 RA: 07:13:32.32 DEC: -44:38:23.1 Eq 2000.0 Offs: +0.0 -0.3  
 Unknown tau: 0.547 Tsys: 953. Time: 3.7 min El: 64.9  
 N: 1652 l0: 826.473 V0: 33.10 Dv: 0.6351 LSR  
 F0: 691473.062 Df: -1.465 Fi: 679471.452  
 Bef: 1.0 Fef: 0.95 Gim: 0.1000  
 H2O : 0.3460 Pamb: 553.4 Tamb: 269.3 Tchop: 289.3 Tcold: 72.6  
 Tatm: 0.0 Tau: 0.547 Tatm i: 0.0 Tau i: 0.427  
 61346,

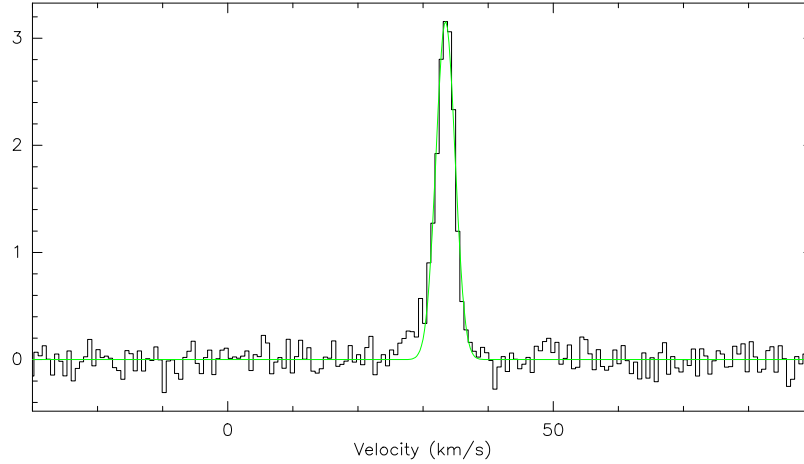


Figure 5: L02-pup CO(6-5) spectrum

1908; 1 RAFGL3068 CO(6-5) AP-C604-AF02 O:23-OCT-2009 R:23-OCT-2009  
 RA: 23:19:12.39 DEC: 17:11:35.4 Eq 2000.0 Offs: +0.6 -0.2  
 Unknown tau: 0.726 Tsys: 1306. Time: 5.0 min El: 47.5  
 N: 6608 l0: 3304.39 V0: -31.00 Dv: 0.1588 LSR  
 F0: 691473.076 Df: -0.3662 Fi: 679473.947  
 Bef: 1.0 Fef: 0.95 Gim: 0.1000  
 H2O : 0.4662 Pamb: 553.6 Tamb: 270.5 Tchop: 288.4 Tcold: 72.6  
 Tatm: 0.0 Tau: 0.726 Tatm i: 0.0 Tau i: 0.548  
 73582, 73584,

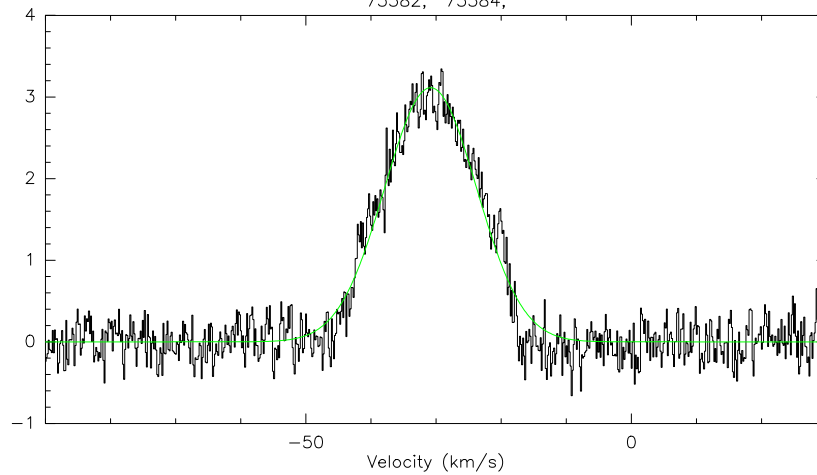


Figure 6: RAFGL-3068 CO(6-5) spectrum

2930; 1 R-HOR CO(6-5) AP-C604-AF02 O:10-NOV-2008 R:10-NOV-2008  
 RA: 02:53:52.80 DEC: -49:53:23.0 Eq 2000.0 Offs: +0.0 +0.2  
 Unknown tau: 0.658 Tsys: 2320. Time: 7.4 min El: 24.8  
 N: 1652 l0: 826.473 V0: 35.70 Dv: 0.6351 LSR  
 F0: 691473.062 Df: -1.465 Fi: 679470.670  
 Bef: 1.0 Fef: 0.95 Gim: 0.1000  
 H2O : 0.4524 Pamb: 554.6 Tamb: 271.6 Tchop: 289.3 Tcold: 72.6  
 Tatm: 0.0 Tau: 0.658 Tatm i: 0.0 Tau i: 0.530  
 60949, 60951,

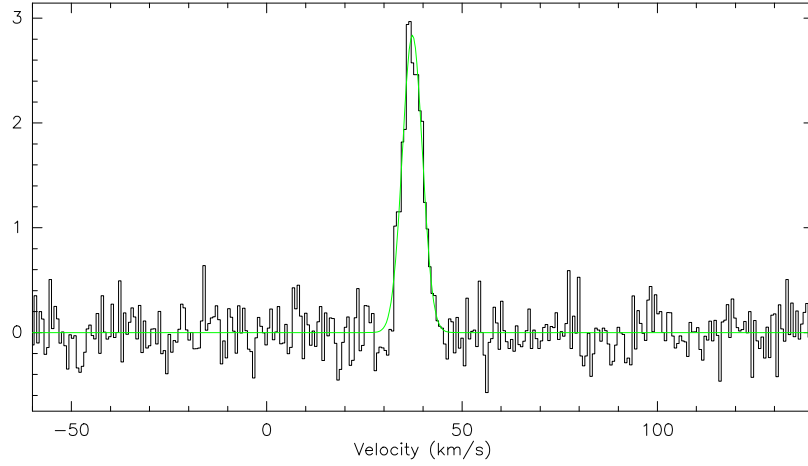


Figure 7: R-HOR CO(6-5) spectrum

732; 1 IRAS15194-51 CO(6-5) AP-C604-AF02 O:17-JUN-2009 R:17-JUN-2009  
 l: 0.000 b: 0.000 Ho Offs: -0.1 -0.1  
 Unknown tau: 0.827 Tsys: 1394. Time: 0.12 min El: 56.7  
 N: 1924 l0: 962.815 V0: -15.00 Dv: 0.6351 LSR  
 F0: 691473.062 Df: -1.465 Fi: 679473.291  
 Bef: 1.0 Fef: 0.95 Gim: 0.1000  
 H2O : 0.5007 Pamb: 554.1 Tamb: 265.0 Tchop: 288.6 Tcold: 72.8  
 Tatm: 0.0 Tau: 0.827 Tatm i: 0.0 Tau i: 0.617  
 33215,

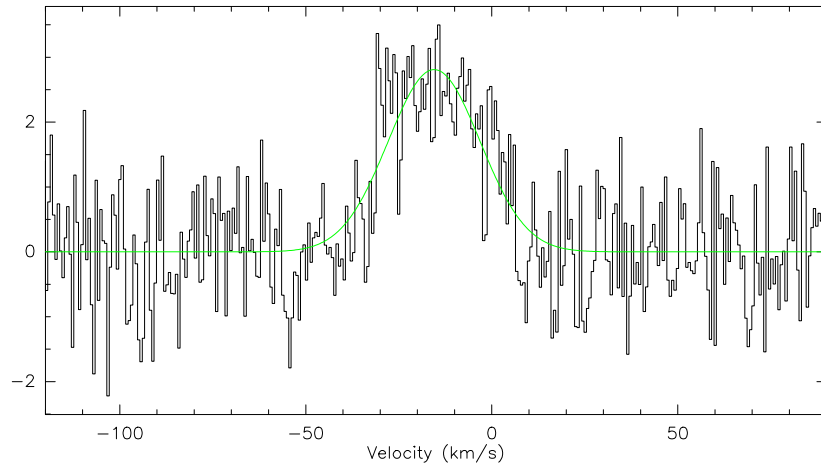


Figure 8: IRAS-15194 CO(6-5) spectrum

214960; 2 IK-TAU CO(6-5) AP-C604-AF02 0:22-OCT-2009 R:25-OCT-2009  
 RA: 03:53:28.89 DEC: 11:24:21.8 Eq 2000.0 Offs: -0.0 -0.7  
 Unknown tau: 0.804 Tsys: 1846. Time: 5.0 min El: 41.6  
 N: 6607 l0: 3304.14 V0: 34.00 Dv: 0.1588 LSR  
 F0: 691473.076 Df: -0.3662 Fi: 679471.806  
 Bef: 1.0 Fef: 0.95 Gim: 0.1000  
 H2O : 0.5386 Pamb: 554.3 Tamb: 269.6 Tchop: 288.4 Tcold: 72.6  
 Tatm: 0.0 Tau: 0.804 Tatm i: 0.0 Tau i: 0.631  
 73253,

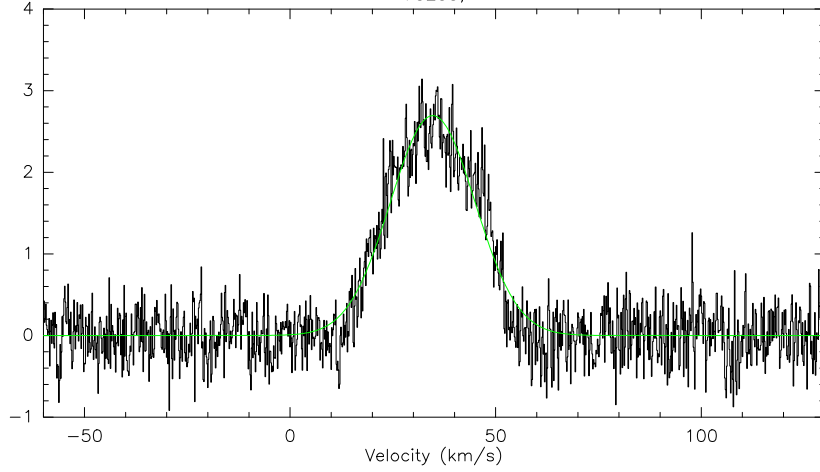


Figure 9: IK-TAU co(6-5) spectrum

4092; 1 R-AND CO(6-5) AP-C604-AF02 0:24-OCT-2009 R:24-OCT-2009  
 RA: 00:24:01.93 DEC: 38:34:37.1 Eq 2000.0 Offs: +0.6 -0.2  
 Unknown tau: 0.763 Tsys: 2775. Time: 7.5 min El: 28.2  
 N: 6607 l0: 3304.14 V0: -16.00 Dv: 0.1588 LSR  
 F0: 691473.076 Df: -0.3662 Fi: 679473.758  
 Bef: 1.0 Fef: 0.95 Gim: 0.1000  
 H2O : 0.5045 Pamb: 554.2 Tamb: 268.9 Tchop: 288.5 Tcold: 72.6  
 Tatm: 0.0 Tau: 0.763 Tatm i: 0.0 Tau i: 0.598  
 73965, 73968, 73970,

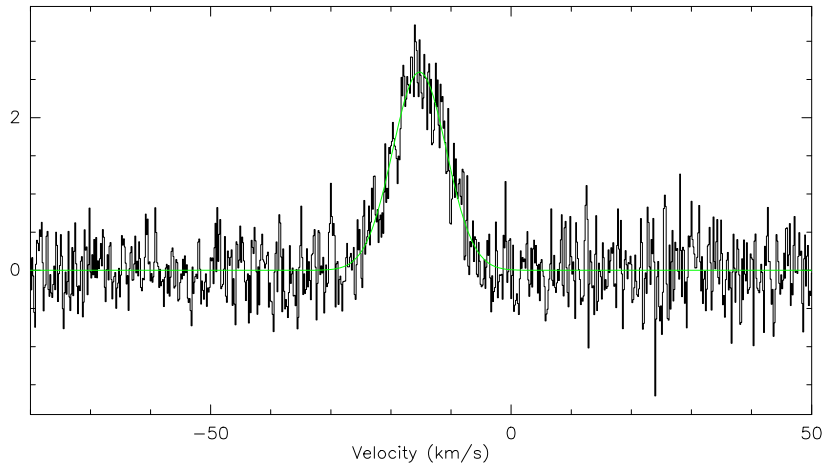


Figure 10: R-And CO(6-5) spectrum

5166; 2 07454-7112 CO(6-5) AP-C604-AF02 0:11-NOV-2008 R:03-DEC-2009  
 RA: 07:45:02.82 DEC: -71:19:42.2 Eq 2000.0 Offs: +0.0 -0.9  
 Unknown tau: 0.703 Tsys: 1498. Time: 2.7 min El: 25.4  
 N: 6608 IO: 3304.39 V0: -39.00 Dv: 0.1588 LSR  
 F0: 691473.062 Df: -0.3662 Fi: 679474.081  
 Bef: 1.0 Fef: 0.95 Gim: 0.1000  
 H2O : 0.4854 Pamb: 554.6 Tamb: 273.6 Tchop: 289.5 Tcold: 72.6  
 Tatm: 0.0 Tau: 0.703 Tatm i: 0.0 Tau i: 0.553  
 61378, 61389, 61408, 61447,

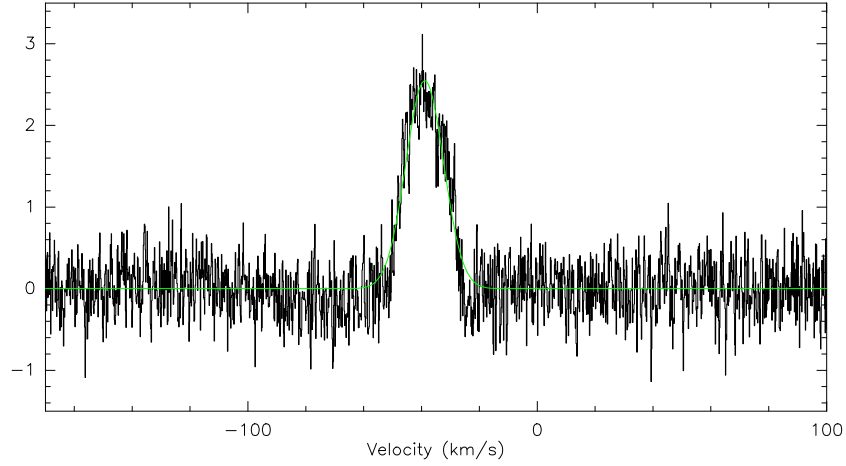


Figure 11: 07454-7211 CO(6-5) spectrum

256; 2 W-AQL CO(6-5) AP-C604-AF02 0:21-OCT-2009 R:25-OCT-2009  
 RA: 19:15:23.36 DEC: -07:02:50.4 Eq 2000.0 Offs: +0.1 -0.0  
 Unknown tau: 1.193 Tsys: 2289. Time: 1.2 min El: 68.4  
 N: 1925 IO: 963.473 V0: -24.00 Dv: 0.6351 LSR  
 F0: 691473.076 Df: -1.465 Fi: 679473.508  
 Bef: 1.0 Fef: 0.95 Gim: 0.1000  
 H2O : 0.9115 Pamb: 553.8 Tamb: 274.4 Tchop: 287.1 Tcold: 72.6  
 Tatm: 0.0 Tau: 1.193 Tatm i: 0.0 Tau i: 0.978  
 73141, 73147,

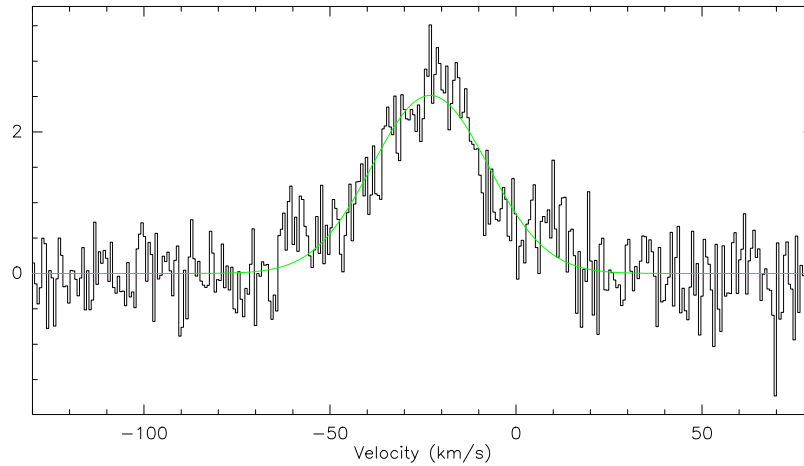


Figure 12: W-Aql CO(6-5) spectrum

1124; 1 PI1-GRU CO(6-5) AP-C604-AF02 O:17-JUN-2009 R:17-JUN-2009  
 RA: 22:22:44.22 DEC: -45:56:52.6 Eq 2000.0 Offs: +0.1 -0.1  
 Unknown tau: 1.016 Tsys: 1701. Time: 2.0 min El: 63.2  
 N: 1925 IO: 962.940 VO: -12.00 Dv: 0.6351 LSR  
 FO: 691473.062 Df: -1.465 Fi: 679474.244  
 Bef: 1.0 Fef: 0.95 Gim: 0.1000  
 H2O : 0.6983 Pamb: 553.4 Tamb: 265.1 Tchop: 289.0 Tcold: 72.7  
 Tatm: 0.0 Tau: 1.016 Tatm i: 0.0 Tau i: 0.831  
 33353, 33355, 33357,

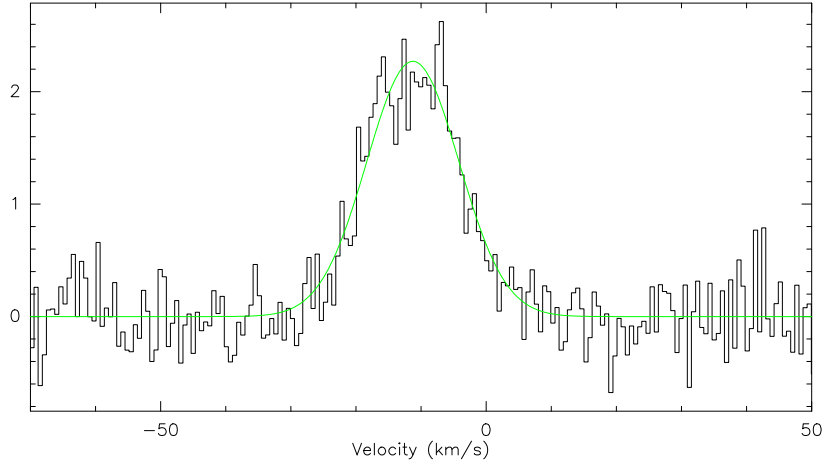


Figure 13: PI1-Gru CO(6-5) spectrum

15320; 1 VYCMa CO(6-5) AP-C604-AF02 O:17-JUN-2009 R:17-JUN-2009  
 RA: 07:22:58.33 DEC: -25:46:03.2 Eq 2000.0 Offs: -2.0 -3.4  
 Unknown tau: 1.032 Tsys: 1883. Time: 4.0 min El: 78.7  
 N: 1789 IO: 895.207 VO: 0.000 Dv: 0.6351 LSR  
 FO: 691473.062 Df: -1.465 Fi: 679471.884  
 Bef: 1.0 Fef: 0.95 Gim: 0.1000  
 H2O : 0.7397 Pamb: 554.5 Tamb: 270.5 Tchop: 288.4 Tcold: 72.6  
 Tatm: 0.0 Tau: 1.032 Tatm i: 0.0 Tau i: 0.836  
 33432,

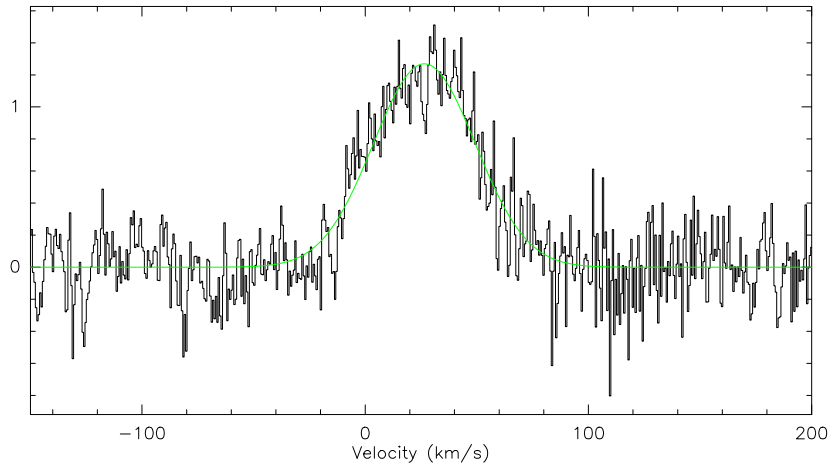


Figure 14: VYCMa CO(6-5) spectrum, probably not properly focused.

3178; 1 V-HYA CO(6-5) AP-C604-AF02 0:11-NOV-2008 R:11-NOV-2008  
 l: 0.000 b: 0.000 Ho Offs: +0.1 -0.0  
 Unknown tau: 0.558 Tsys: 980. Time: 0.33 min El: 63.4  
 N: 3303 l0: 1652.20 V0: -16.50 Dv: 0.3175 LSR  
 F0: 691473.062 Df: -0.7324 Fi: 679474.290  
 Bef: 1.0 Fef: 0.95 Gim: 0.1000  
 H2O : 0.3369 Pamb: 553.5 Tamb: 269.1 Tchop: 289.3 Tcold: 72.6  
 Tatm: 0.0 Tau: 0.558 Tatm i: 0.0 Tau i: 0.418  
 61365,

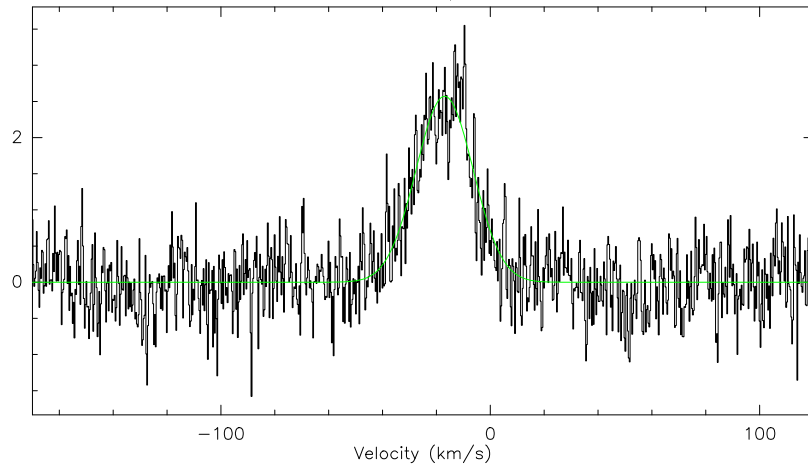


Figure 15: V-Hya co(6-5) spectrum. Pointing offset of 3'' from central position.

816; 2 TX-PSC CO(6-5) AP-C604-AF01 0:24-OCT-2009 R:03-DEC-2009  
 l: 0.000 b: 0.000 Ho Offs: -0.0 -7.6  
 Unknown tau: 0.960 Tsys: 2003. Time: 1.0 min El: 55.7  
 N: 1652 l0: 826.473 V0: 13.00 Dv: 0.6351 LSR  
 F0: 691473.076 Df: -1.465 Fi: 679471.984  
 Bef: 1.0 Fef: 0.95 Gim: 0.1000  
 H2O : 0.7148 Pamb: 554.1 Tamb: 266.1 Tchop: 288.3 Tcold: 72.6  
 Tatm: 0.0 Tau: 0.960 Tatm i: 0.0 Tau i: 0.844  
 73916- 73917,

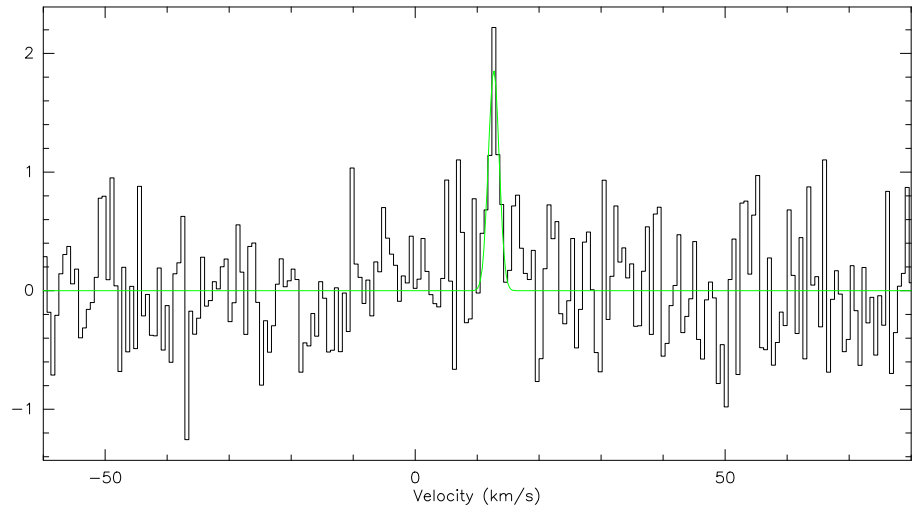


Figure 16: TX-Psc co(6-5) spectrum. Not properly pointed.

1908; 1 WX-PSC CO(6-5) AP-C604-AF02 0:24-OCT-2009 R:24-OCT-2009  
 RA: 01:06:25.98 DEC: 12:35:53.0 Eq 2000.0 Offs: +1.0 -0.4  
 Unknown tau: 0.766 Tsys: 1707. Time: 11. min El: 51.5  
 N: 3303 l0: 1652.07 V0: 9.000 Dv: 0.3175 LSR  
 F0: 691473.076 Df: -0.7324 Fi: 679472.387  
 Bef: 1.0 Fef: 0.95 Gim: 0.1000  
 H2O : 0.5187 Pamb: 554.4 Tamb: 268.4 Tchop: 288.4 Tcold: 72.6  
 Tatm: 0.0 Tau: 0.766 Tatm i: 0.0 Tau i: 0.616  
 73924, 73926, 73955, 73957, 73959,

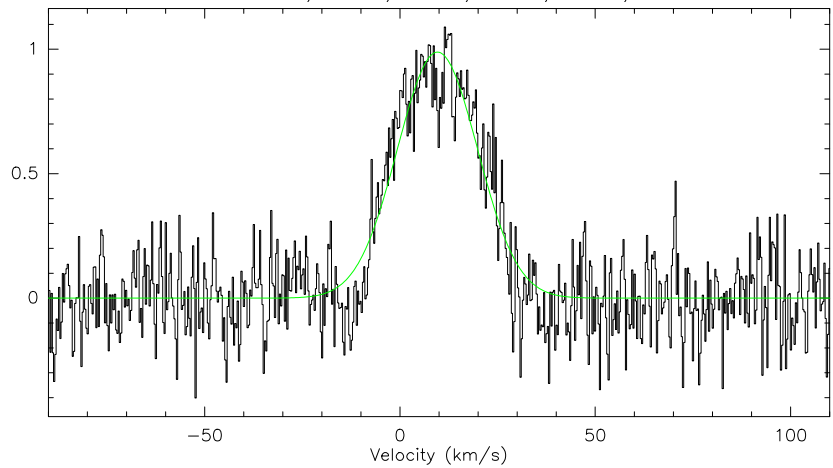


Figure 17: WX-Psc co(6-5) spectrum



3196; 1 R-SCL CO(6-5) AP-C604-AF02 0:23-OCT-2009 R:23-OCT-2009  
 RA: 01:26:58.09 DEC: -32:32:35.6 Eq 2000.0 Offs: -0.2 -0.3  
 Unknown tau: 0.684 Tsys: 1025. Time: 5.0 min El: 77.1  
 N: 3303 l0: 1652.20 V0: -19.00 Dv: 0.3175 LSR  
 F0: 691473.076 Df: -0.7324 Fi: 679473.013  
 Bef: 1.0 Fef: 0.95 Gim: 0.1000  
 H2O : 0.4608 Pamb: 553.5 Tamb: 268.7 Tchop: 288.0 Tcold: 72.6  
 Tatm: 0.0 Tau: 0.684 Tatm i: 0.0 Tau i: 0.552  
 73591, 73593,

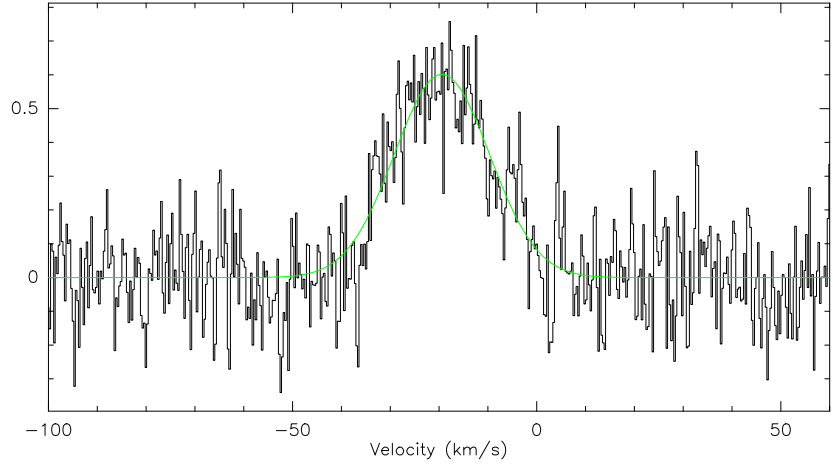


Figure 18: R-Scl co(6-5) spectrum

6360; 1 R-FOR CO(6-5) AP-C604-AF02 0:24-OCT-2009 R:24-OCT-2009  
 RA: 02:29:15.31 DEC: -26:05:55.7 Eq 2000.0 Offs: -0.2 -0.6  
 Unknown tau: 0.757 Tsys: 1150. Time: 12. min El: 80.1  
 N: 3303 l0: 1652.07 V0: -2.000 Dv: 0.3175 LSR  
 F0: 691473.076 Df: -0.7324 Fi: 679472.495  
 Bef: 1.0 Fef: 0.95 Gim: 0.1000  
 H2O : 0.5182 Pamb: 554.0 Tamb: 269.2 Tchop: 288.2 Tcold: 72.7  
 Tatm: 0.0 Tau: 0.757 Tatm i: 0.0 Tau i: 0.611  
 73978- 73979, 73981- 73982, 73984,

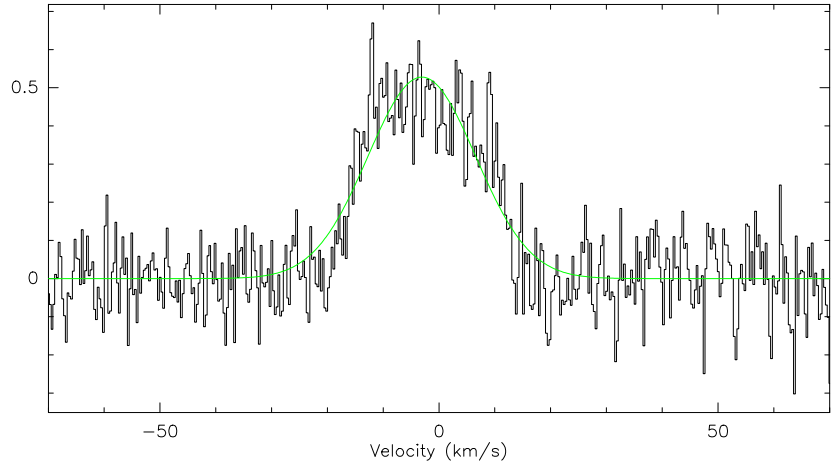
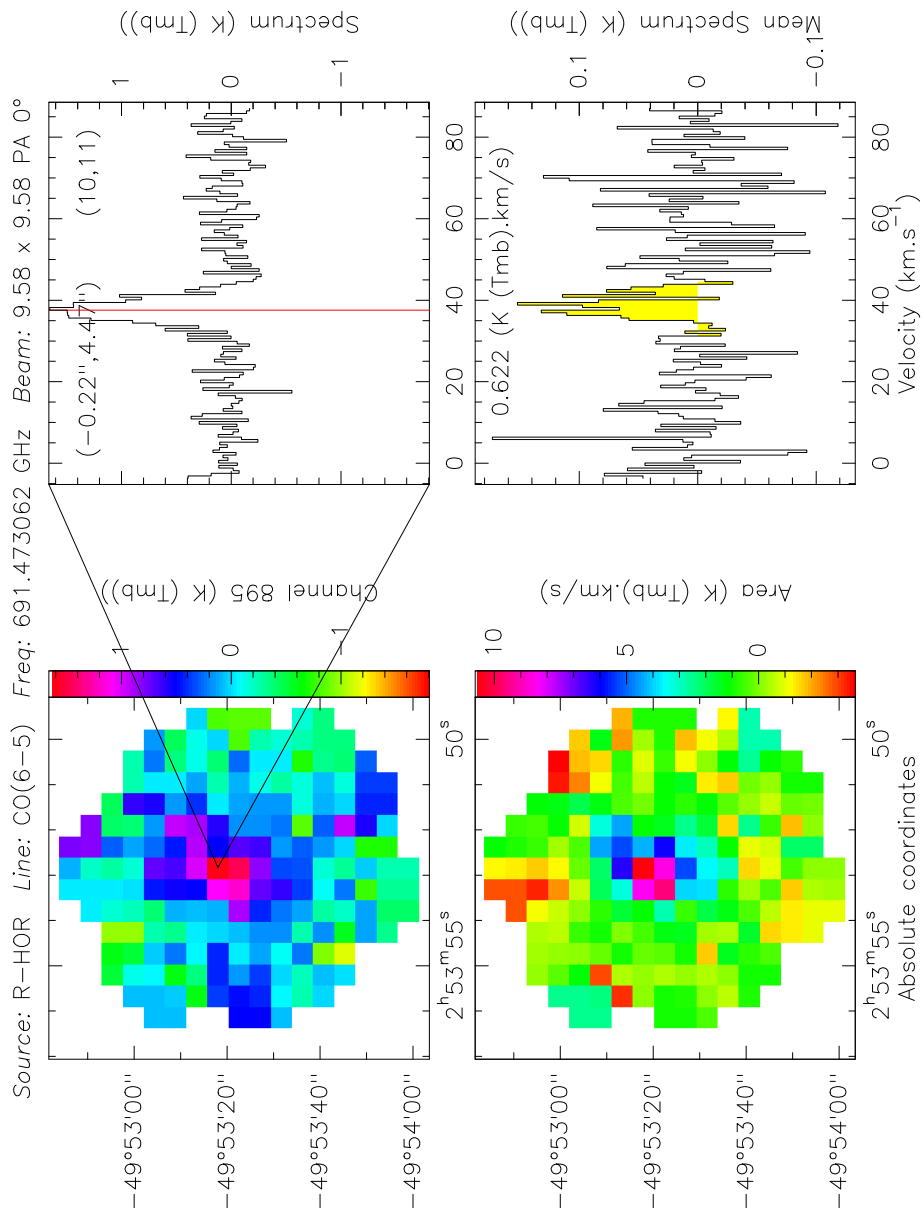
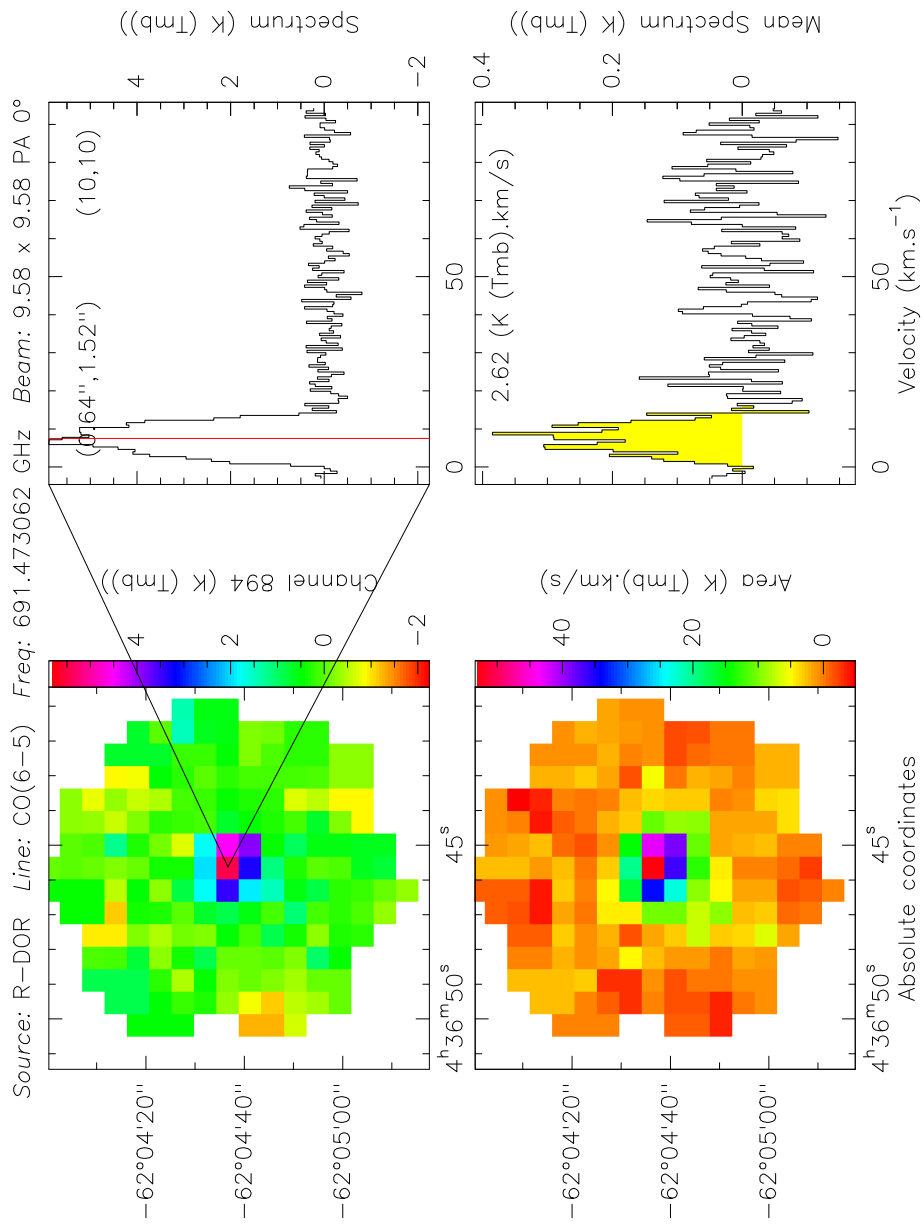


Figure 19: R-For co(6-5) spectrum



dcdc.lmvp

Figure 20: R-HOR co(6-5) map



dml:xdpx

Figure 21: R-DOR co(6-5) map



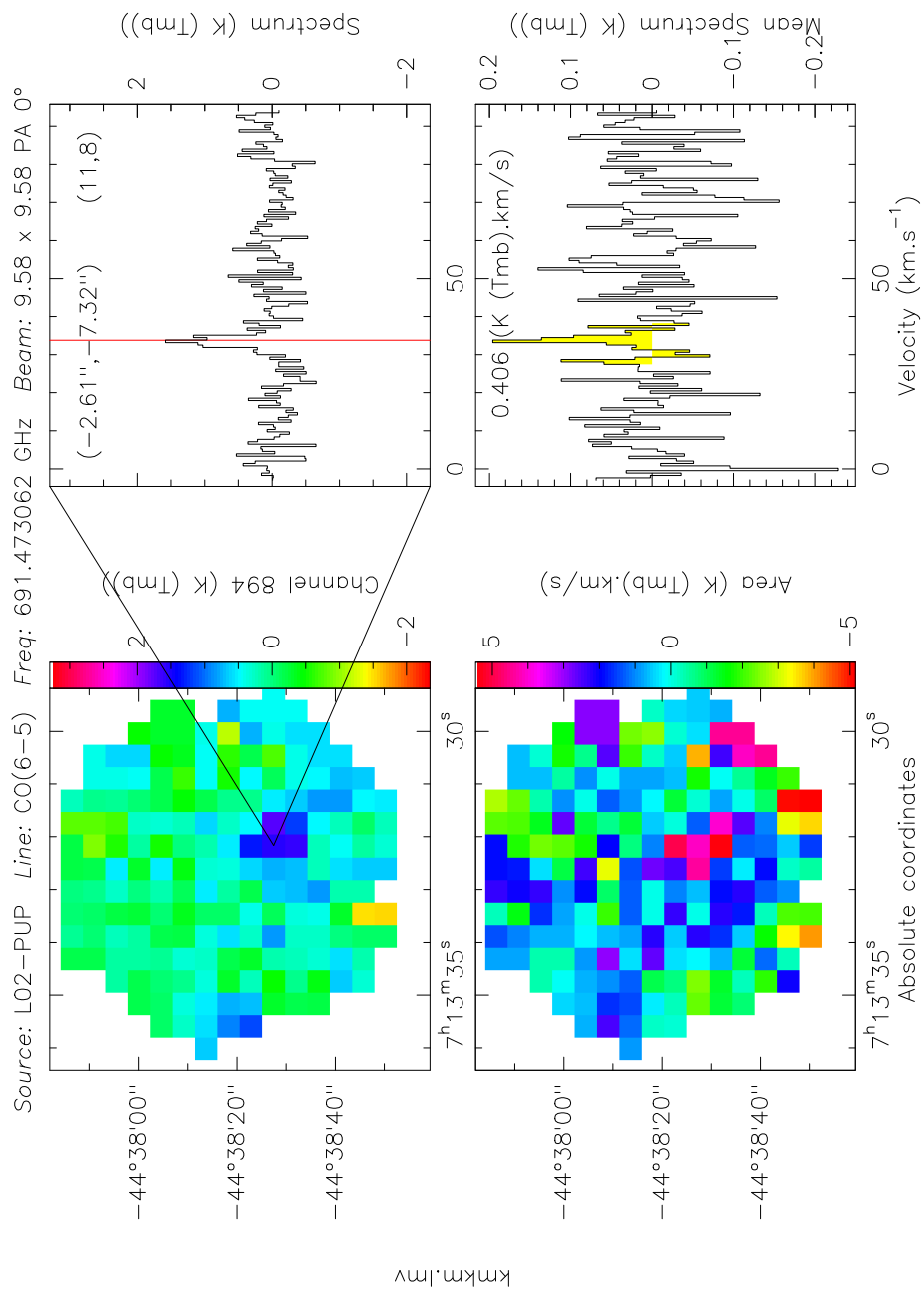


Figure 23: L02-pup mapping in co(6-5)

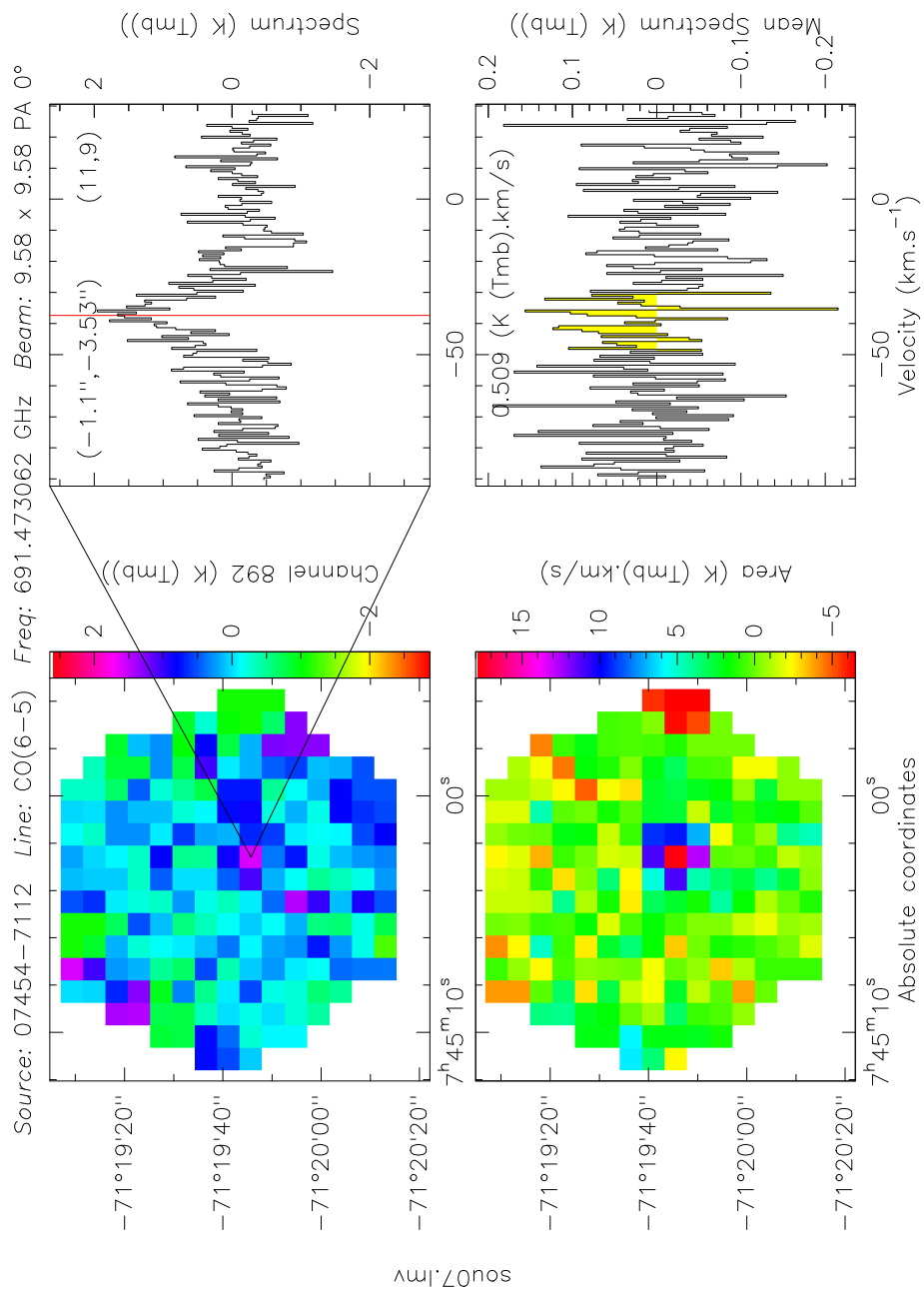
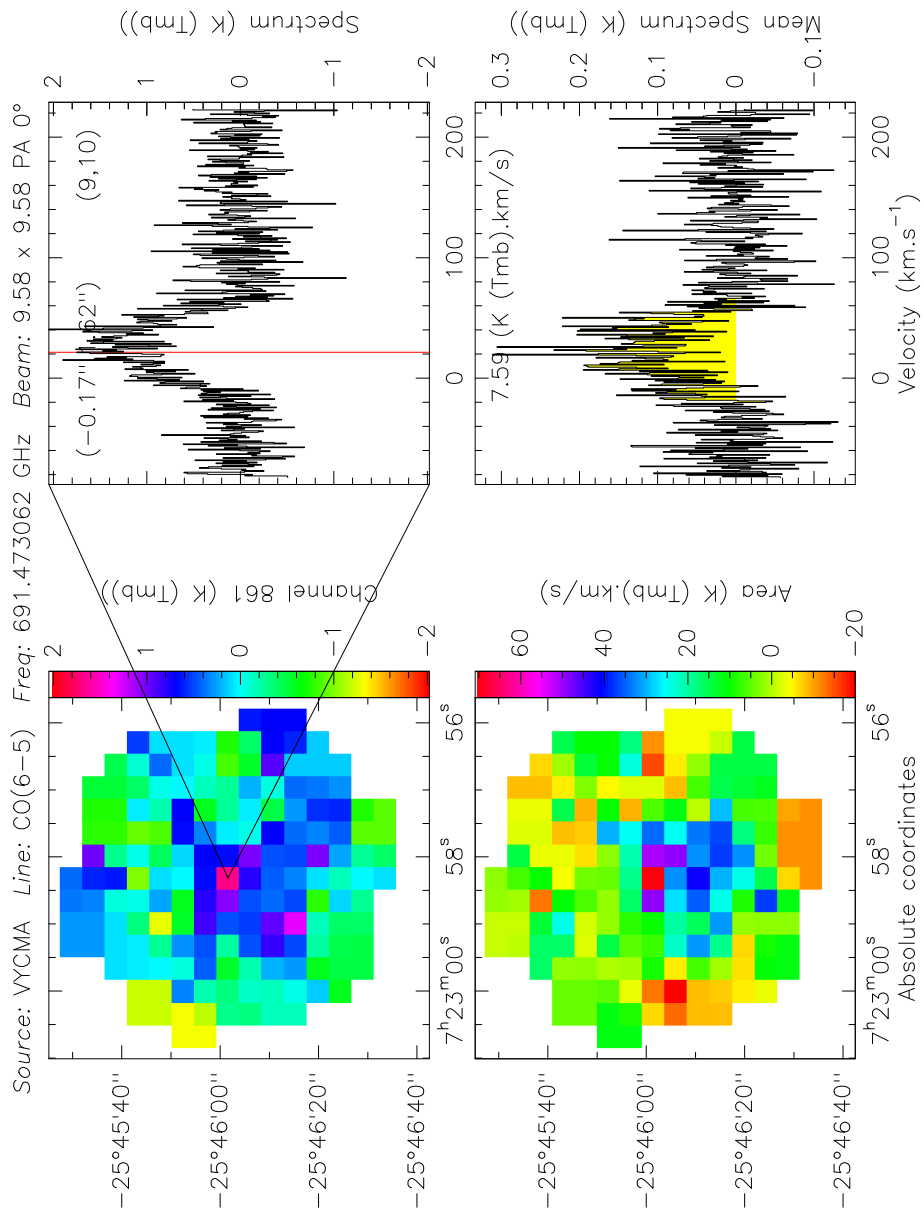


Figure 24: 07454 mapping in co(6-5)



son vycma.lmv

Figure 25: VY-CMA map, extended structure? focus problem during day-time?